Proceedings of ASME Turbo Expo 2008: Power for Land, Sea and Air
GT2008
June 9-13, 2008, Berlin, Germany

GT2008-50492

IMPROVING THE ACCURACY OF MULTIHOLE PROBE MEASUREMENTS IN VELOCITY GRADIENTS

Valery Chernoray
Department of Applied Mechanics
Chalmers University of Technology
412 96 Gothenburg, Sweden
valery.chernoray@chalmers.se

Johan Hjärne
Department of Aero and Thermo Dynamics
Volvo Aero Corporation
461 81 Trollhättan, Sweden
johan.hjarne@volvo.com

ABSTRACT

This study describes an implementation and verification of an effective and reliable correction for the finite-size effects of pressure probes. A modified version of correction by Ligrani *et al.* (*Exp. Fluids*, vol. 7, 1989, p. 424) was used. It is shown that the correction procedure can be implemented in two steps as in Ligrani *et al*. or in a single step, either for probe pressures, or for velocity components. The latter correction method is found to have the best performance and studied in very detail. The effect of the correction in application to the highly three-dimensional flow downstream of the outlet guide vanes is scrutinized through detailed side-by-side comparison with corresponding cross hot-wire data. The influence of the correction on all three velocity components, flow streamlines and streamwise vorticity fields is thoroughly examined. Two flow cases with different incoming turbulence intensities are considered. The study demonstrates a very good efficiency and reliability of the correction, which lead to a significant improvement of the corrected velocity data. The improvement in crossflow velocity components has allowed correct description of the flow streamlines, and as a result, the secondary flow field structures were resolved more accurately. The considered correction does not affect the streamwise vorticity component, which is clarified as well. A very important fact is that the correction is not found to over-correct and distort the data, thus can be used safely. A very good performance of the correction for the finite-size effects of pressure probes presented in this study allows us to recommend it as a mandatory step in postprocessing procedures for multihole pressure probes.

1 INTRODUCTION

Multihole pressure probes are widely used as accurate, robust, and versatile flow-measuring instruments with numerous advantages over other flow measuring devices. These probes are very common in gas turbine experiments and often used in strong gradient fields, e.g. traversing wakes or shocks. Surprisingly, though, very few experimentalists who use multihole pressure probes apply the spatial resolution and downwash velocity corrections in such situations.

In experiments performed in a low pressure turbine outlet guide vane (OGV) cascade at Chalmers University by Hjärne *et al.* [2, 3, 4], Kennedy [5], and Kennedy *et al.* [6] the five-hole probe measurement data were complemented with the cross hot-wire measurements. After analyzing the data it was found that the crossflow velocity components measured by the five-hole pressure probes disagreed with those obtained by the cross hot-wires. The differences between these two measurement data sets were observed in the zones of vane wakes and sidewall boundary layers where velocity gradients are strong. Subsequent research has revealed that the correction by Ligrani *et al.* [1] can be used to compensate for the 5-hole probe errors caused by the velocity gradients. The correction procedure by Ligrani *et al.* [1] was modified, and the implementation and verification of the correction is described in the current paper. The efficiency of the obtained correction was scrutinized through detailed side-by-side comparison with corresponding cross hot-wire data. To our knowledge, such verifications were not performed previously. A very important fact is that the described correction is not found to over-correct and distort the data and can be used safely.

The correction was found to have a very good performance and reliability and can be recommended for use in situations when the probe size poses the problem of spatial resolution. Especially it can be useful in experiments with modern advanced probes such as fast response probes with embedded sensors, or 12- and 16-hole probes [7-11]. These probes usually have relatively large heads and improved spatial resolution can therefore only be obtained by correcting the measurement data. Moreover, it can be noted that the spatial resolution errors are

unavoidable even for very small probes if the gradients in the flow are strong. Improvement for the crossflow velocity components can always be obtained, and in the most recent of our studies (e.g. [12]) this correction is always used. Authors recommend the described correction as a mandatory step in all data postprocessing procedures for multi-hole pressure probes.

2 NOMENCLATURE

C	blade chord [m]
Re	Reynolds number based on chord length
x, y, z	coordinates [m], see Figure 1
U, V, W	mean velocity components in x, y and z-directions [m/s]
U_{FS}	mean streamwise velocity in the free-stream (in potential core between the vanes)
Δ	correction constant [m]
d	probe diameter [m]
K	nondimensional velocity gradient
Cp	nondimensional pressure coefficient
ω_x	streamwise vorticity [1/s]
OGV	outlet guide vane

3 EXPERIMENTAL SETUP

3.1 The Test Facility:

The experiments were performed in a linear cascade facility at Chalmers University. This facility is of open circuit blower type and operates at a realistic Reynolds number range (Re ~ 300,000) for OGV flows. The cross section of the working part of the facility is 200 by 1200 mm and the inlet velocity in the cascade is 20 m/s. The cascade is designed and developed in the frame of a longtime research project and used in several years for validation of numerical tools, and for gaining an increased understanding of the detailed aerodynamics around OGVs, including secondary flows and separation margins. The design and validation of the facility is described in detail by Hjärne *et al.* [13-15], and Hjärne [4].

This test-facility consists of a wide-angle diffuser, a settling chamber, a contraction and a test section which was equipped with an end-wall boundary-layer suction system. A 30 kW fan is used to drive the flow through a diffuser and a flow conditioner (consisting of a honeycomb and three screens with different porosity). Working incidence angles are designed to vary between 0 and 52 degrees relative to the axial inlet flow angle. Seven vanes are designed in the test-section to fulfill good flow periodicity.

To vary the incoming flow turbulence intensity a turbulence grid was placed 450 mm upstream of the cascade and parallel to the leading edge plane, see Figure 1. Without the grid the turbulence intensity was approximately 0.5% and the grid increased the turbulence intensity to 5%.

Two traversing systems have been used to measure the flow field both upstream and downstream. The movements in the (y, z) plane are controlled by stepper motors with an accuracy of at least 12.5 µm. As the test rig has very good symmetry, the outlet measurements were taken over half of the span one pitch length over the central blade at three different streamwise locations downstream of the trailing edge (0.25C, 0.5C and 0.8C). A discretization of 2 mm in yz-directions was used and over 4000 spatial points were measured in each plane. To avoid wall proximity effects, as suggested in [16], the flow field was not measured at a distance closer than two times the five-hole probe head size to the endwall. The same measuring planes were used for both the five-hole probe and the cross hot-wire probe measurements.

All measurements were controlled by a PC and sampling and saving of data was done with the LabVIEW software. This software was also used for the automated flow measurements using a traversing system connected to a pre-defined mesh of sampling points. Post processing of the experimental data was performed in the Matlab software package.

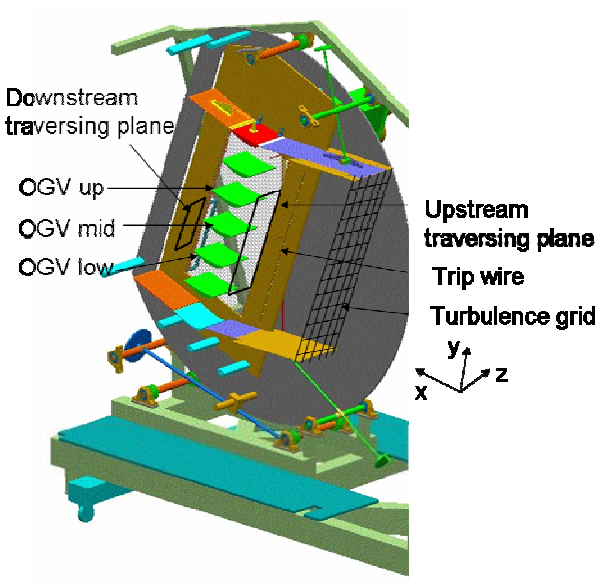

Figure 1 Test section of the experimental facility.

3.2 Cross Hot-Wire Measurement Procedure:

The cross hot-wire array was a standard Dantec cross-wire probe equipped with gold plated 5-µm wires of 1.2-mm active length and distance between the wires of 1 mm. The calibration of the cross-wire probe was performed using a calibration facility. The calibration system consists of a low turbulent jet and an automated angular traversing mechanism. The probe rotation is performed by servo motors with optical encoders, which provide the resolution of angular positioning of 1/80 degree. The hot-wire probe was calibrated at ten different velocities between 2 and 35 m/s for flow angles between ±45 degrees with resolution of 5 degrees. The velocity of the calibration jet was monitored by a FCO510 digital micromanometer.

For the cross wire measurements the acquisition system used was a 16-bit, 16 channel Iotech Wavebook. During the measurements 1000 data samples were acquired at 500 Hz rate in every spatial point. The optimal sampling rate was determined from the auto-correlation coefficient function and the subsequently computed integral time scale. The sampling time was defined from a compromise between the good statistics and realistic run times. A highest statistical uncertainty for the mean velocity is estimated as 1.63% with 99% confidence for the regions with the highest turbulence intensity (20%, in the wakes).

The hot-wires were operated by Dantec's DISA 56C17 dual-channel anemometer at overheat ratio of 1.8. The anemometer bandwidth was adjusted by using the squire wave test to approximately 30 kHz. The hot-wire signal was band pass filtered between 30 Hz and 30 kHz. Both filtered and unfiltered signals were acquired during the measurements.

The voltages from the two wires of the cross-wire probe were converted to the velocity components using the two-dimensional cubic interpolation (*griddata* function in Matlab) over the calibration map. After the conversion, the achieved velocity traces were time averaged. Because of a finite distance between the wires the measurements from the cross hot-wire probe have required a spatial correction. Thus, the obtained in the previous step *mean* velocities were backward converted using the calibration map to *mean* voltages. Then the voltages for one of the wires were interpolated as if this wire is located in same spatial location as the second wire, and another conversion to velocities gave the final corrected data.

To obtain both crossflow velocity components, V and W, the measurements were performed twice in each measurement plane; and in the second run the probe was turned 90° around its axis.

The ambient temperature was constantly monitored during the experiments, and the changes in temperature were within ±0.5°. To maintain constant wire overheat and to compensate for the ambient temperature change the operating temperature of the hot-wires was fine-adjusted at the beginning of each run. A reference voltage was taken during calibration and the bridges adjusted accordingly to match. In addition to this, the velocity could also be measured during the experimental set-up in a specially chosen reference point, thus the velocity at this point could be matched to the actual velocity to account for the temperature changes. The reference velocity was obtained using the five-hole probe and the reference point was chosen in a potential core between the vanes at a position with zero pitch and yaw angles.

3.3 Measurement Procedure for the Five-Hole Probe:

The five-hole pressure probe was manufactured at Chalmers, see Figure 2. The size of the probe head diameter is 3.5 mm with individual distances between the holes of 1 mm. The probe was made of five steel tubes of 1 mm external and 0.8 mm internal diameter. The probe tip half cone angle is 45 degrees. The probe calibration was performed in the same pitch-roll calibration system as the cross-wires (see description above) at a velocity of 20 m/s for 408 angular positions. The probe was pitched between –20 and 20 degrees and rotated around the longitudinal axis in 0-180 degree range with resolution of 2.5 degrees for both angular directions.

Prior to the calibration the probe was aligned in the calibration facility using the so-called non-nulling approach. The probe was rotated along its axis and the port pressures were monitored for different roll angles. The probe was considered perfectly aligned with the calibration jet when the port pressures did not change during the axial rotation. For an aligned probe the pressures were not necessarily equal for all peripheral ports due to the minor probe asymmetries. The nulling method (when the probe alignment is performed by equaling the opposite pressure ports) was not used here since it is valid only for perfectly symmetric probes.

During the measurements the pressures from the probe were monitored by a 16-channel PSI 9116 digital pressure scanner (Pressure System Inc.) with a measuring range of 2500 Pa and an accuracy better than ±3.75 Pa. The scanner performs channel scan at fixed frequency of 500 Hz. In every spatial point 500 data samples were taken. Only mean pressures from 5-hole probe were recorded. The sampling settings resulted in a statistical uncertainty of 0.45 Pa with 99% confidence for the regions with the highest turbulence intensity (20%, in the wakes).

Five-hole probe data conversion was performed using the method of "the local least squares". During the calibration the non-dimensional pressure coefficients are computed, and obtained functional relationships are fitted by the polynomials covering the entire calibration range. The procedure of sectoring was not used here, since the entire calibration range was relatively narrow, covering only one, central sector. The non-dimensional pressure coefficients were defined in a standard way, as described e.g. by Pisasale and Ahmed [17]. The fitting with the calibration polynomials resulted in errors less than ±0.2 m/s for all velocity components. A more detailed error analysis and calibration maps are presented in Hjärne [4]. The probe spatial resolution correction and the downwash correction are described in detail in the next paragraph.

Figure 2 Photograph of conical 5-hole probe.

4 MULTIHOLE PROBE CORRECTIONS

A finite size of a multihole probe leads to the erroneous measurements in flows with spatial gradients. The errors are unavoidable even for very small probes if the spatial gradients are strong. Two error sources are known: (1) the probe resolution error arises since the probe ports are spatially separated, thus different ports are located in different parts of the flow, and (2) the probe is deflecting the incoming streamlines. The wall proximity effect and the probe blockage effect can also be of great importance though not considered here. The wall effect is seen when the probe is stationed within two diameters from a solid boundary and the blockage from the probe occurs during the measurements in relatively small ducts [16]. Such situations were avoided here.

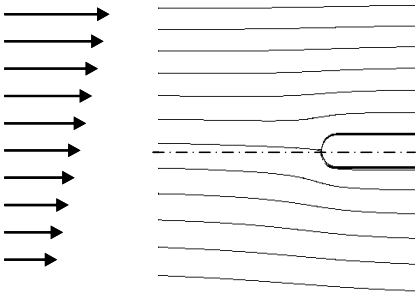

Figure 3 Flow deflection near probe in velocity gradient.

The deflection of the flow by a probe is illustrated in Figure 3. This diagram shows a probe with the contours of total pressure around it. At regions with lager velocities the stagnation pressure is larger, and a flow is set up perpendicular to the main flow direction, from regions of high streamwise velocity to regions of lower streamwise velocity.

4.1 Correction by Ligrani et al.:

The major idea of Ligrani *et al.* [1] is to separate the spatial resolution and the downwash effects and to perform the downwash velocity correction and the spatial resolution correction in two subsequent steps. At the first step Ligrani *et al.* [1] interpolate the pressures from the peripheral ports so that they appear at the location of the central port. This interpolation procedure is implemented at the beginning of the data reduction procedure. At the second step Ligrani *et al.* [1] have implemented the downwash correction for the velocity components measured by a probe by using

$$\frac{V}{U} = \frac{V_{meas}}{U} + \frac{\Delta}{d}\left(\frac{d}{U}\frac{\partial U}{\partial y}\right) \qquad (1)$$

$$\frac{W}{U} = \frac{W_{meas}}{U} + \frac{\Delta}{d}\left(\frac{d}{U}\frac{\partial U}{\partial z}\right) \qquad (2).$$

Here, V_{meas} and W_{meas} represent uncorrected velocities. The original equations by Ligrani *et al.* [1] are rewritten in the dimensionless form to demonstrate that the artificial velocity due to velocity gradient (the second term in each equation) is in fact the nondimensional velocity gradient (bracketed expression) with a proportionality coefficient in front of it. The proportionality coefficient Δ has the dimension of length and Ligrani *et al.* [1] have determined it experimentally.

The method of correction proposed by Ligrani *et al.* [1] was carefully checked and very satisfactory results were obtained as it will be discussed further. However by using some mathematics one can show that the first correction step used by Ligrani *et al.* [1], which involves the interpolation of pressures from the peripheral ports, is in fact almost equivalent to the correction by using Eqs. (1, 2) with a different coefficient Δ. Thus, it seems more convenient to use Eqs. (1, 2) with an adjusted parameter Δ and to avoid the first correction step.

4.2 One-Step Correction for Velocities:

Experiments were performed in a two-dimensional wake to check the hypothesis that the correction for velocities can be modified in such a way so that the first correction step avoided.

The wake in the centerline of the mid vane was measured at three streamwise positions using the cross hot-wire probe and the five-hole probe. Figure 4 shows the nondimensional artificial velocity as a function of the nondimensional velocity gradient *K*. In this figure symbols with different colors are used for data from different streamwise positions (blue — 0.25*C*, green — 0.5*C* and red — 0.8*C*) and crosses and dots are used to denote data sets obtained in runs with different turbulence intensities (crosses — 5 % and dots — 0.5 %). Lines depict linear data fit and prior the fit the data were reflected around the zero point anti-symmetrically to assign the same weights for the positive and negative data.

As is seen from Figure 4 the dependences are in both cases very close to linear and in the case without the preliminary pressure correction (Figure 4, *a*) the data visibly have less scatter. From the slope of the fitting lines on each graph it is possible to obtain the coefficient Δ / d. The value of Δ / d is 0.45 in Figure 4 (*a*) and 0.19 in Figure 4 (*b*). It can be noted that the latter is very close to reported by Ligrani *et al.* [1] value of 0.2. With the pressure port correction applied the sensitivity to velocity gradient is reduced about twice.

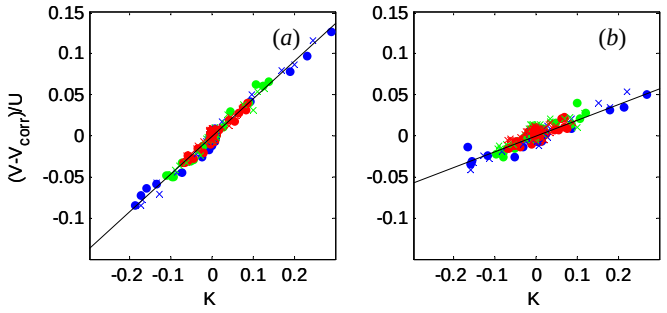

Figure 4 Determination of probe sensitivity to velocity gradient: (*a*) without any preliminary correction, (*b*) after pressure port correction as in Ligrani et al. [1]. Different symbols denote different measurement data sets, see text.

4.3 One-Step Correction for Pressures:

From the fact that the correction for pressures and correction for velocities are equivalent, one can presume that the one-step correction for pressures can be derived as well. By analysing the pressure distribution data on bodies in shear flows (publication [18] for squire cylinder, and our own calculations for conical probes) it was found that the correction for pressures can be performed in the following form

$$Cp_{i,corr} = Cp_i\left(1-2\frac{\Delta_P}{d}\left(\frac{y_i^c}{U}\frac{\partial U}{\partial y}\right)\right) \qquad (3)$$

$$Cp_{i,corr} = Cp_i\left(1-2\frac{\Delta_P}{d}\left(\frac{z_i^c}{U}\frac{\partial U}{\partial z}\right)\right) \qquad (4)$$

Where y_i^c and z_i^c are coordinates of a *i*-peripheral pressure port with respect to the central port, and Δ_P is a correction coefficient which value depends on the shape of pressure probe. The correction coefficient Δ_P / d was derived by using the same experimental data from the two-dimensional wake as in the previous section and optimal value is found close to 1.4.

4.4 Comparison of Corrections:

The efficiency of three different corrections is examined by comparing the reference cross hot-wire data and corrected data from 5-hole probe. In Figure 5 this difference is shown as a function of the nondimensional velocity gradient *K* for data corrected by three different corrections. As previously, symbols with different colors are used for data from different streamwise positions (blue — 0.25*C*, green — 0.5*C* and red — 0.8*C*) and crosses and dots are used to denote data sets obtained in runs with different turbulence intensities (crosses — 5 % and dots — 0.5 %).

It can be observed that the three different corrections perform nearly equally well at moderate velocity gradients and corrections in Figure (*a*) and (*b*) demonstrate somewhat reduced performance at large velocity gradients. The under-correction is largest for the one-step pressure correction. For the correction by Ligrani *et al.* [1] the under-correction lies between the two other corrections. One can note that the one-

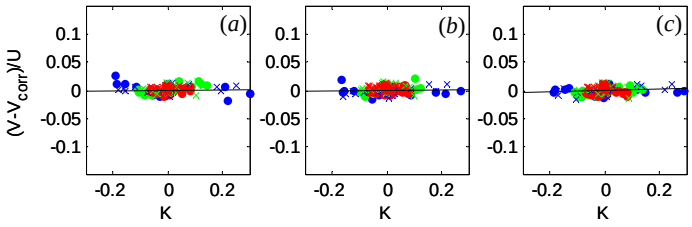

Figure 5 Difference between the reference and corrected vertical velocities in a 2D wake: (*a*) one-step pressure correction, (*b*) correction as in Ligrani *et al.* [1], (*c*) one-step velocity correction. See text for details.

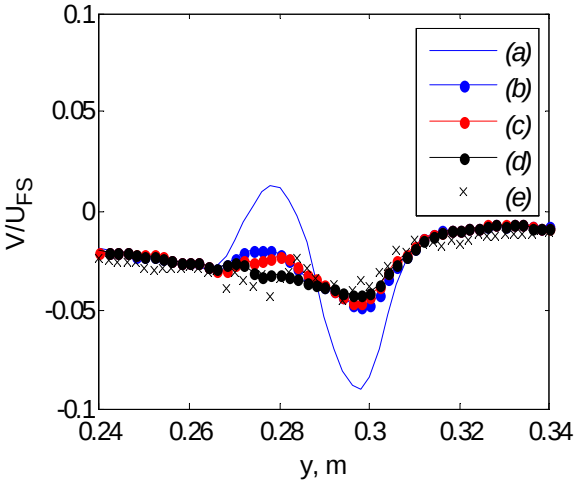

Figure 6 Comparison of effect from three different corrections: (*a*) uncorrected data, (*b*) one-step pressure correction, (*c*) correction as in Ligrani *et al.* [1], (*d*) one-step velocity correction, (*e*) reference data. Profiles of vertical velocity at *x* = 0.5*C*, *z* = -0.036 m.

step velocity correction demonstrates the best performance of all three methods, and it seems that a conclusion can be drawn that the correction performance is improved when the least part of the correction is a "pressure type" correction.

To demonstrate more clearly how the corrections affect the data the corrected velocity profiles are shown in Figure 6 along with the uncorrected and reference data sets. The profiles are obtained at distance *x* = 0.5*C* from the vane trailing edge and at spanwise position *z* = -0.036 m. The flow field for this streamwise station will be examined in detail in the next section of paper. From Figure 6 it follows that the different correction methods perform almost equally well with the best result revealed by the one-step velocity correction. Even though the difference between the three corrections is marginal, the one-step velocity correction seems to perform the best. One can also hypothesize that this correction method is most universal if probes with different shapes are considered.

In next paragraph, the obtained one-step velocity correction is carefully scrutinized. Detailed side-by-side comparison with the cross hot-wire data is performed and the influence of the correction on all three velocity components, flow streamlines and streamwise vorticity fields is thoroughly examined.

5 EXAMINATION OF CORRECTION PERFORMANCE

The correction performance was examined through the side-by-side comparison of the five-hole pressure probe measurements with corresponding data obtained using the cross hot-wires. Two flow cases of different incoming turbulence intensities are considered. Most of the results presented here are for the case of high incoming flow turbulence, and some data from the low-turbulent case are presented at the end part

of the article. It was decided to focus only on the measurements for the streamwise station 0.5*C* behind the OGV, where the velocity gradients are high but not extreme and the hot-wire data are more reliable than at station 0.25*C*.

Figure 7 is presented to give an idea about the flow field behind the OGV. This figure shows the streamwise velocity contours with imposed crossflow velocity arrows. The trailing edge of the guide vane is located at the vertical coordinate y = 0.3 m. This is the central vane of the cascade, and the flow is periodical in the y-direction. Measurements are performed only for the left part for 0 > z > -0.1 and symmetrically reflected around the midspan for additional clarity. The data are from the measurements obtained by the cross hot-wire probe. The velocities are scaled by the velocity in the free-stream U_{FS} which means in the potential core of the flow.

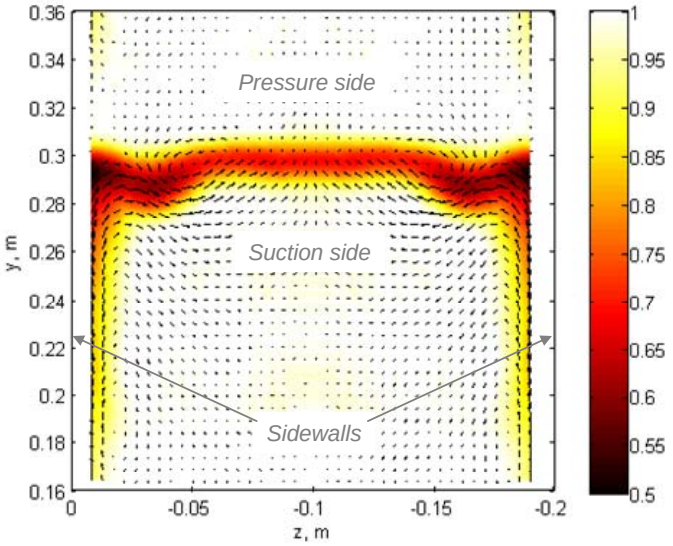

Figure 7 Flow field behind the central OGV at 0.5*C* downstream of the trailing edge. Streamwise velocity U/U_{FS} is shown by contours, and arrows represent crossflow velocity components.

One can note that the flow is essentially three-dimensional. The wake behind the OGV is seen in the central part of the diagram at y = 0.3 m. The wake is formed from the boundary layer vorticity developed on the pressure side and the suction side of the vane which consolidate to one vortex sheet after leaving the OGV. On the side walls the three-dimensional boundary layers are developed. The pressure gradient transports the flow from the pressure side towards the suction side along the end-walls and the boundary layers are also seen to increase in thickness from the pressure side to the suction side. The blade shed vorticity and the boundary layer vorticity are interacting in corners of the vane, forming a well-defined vortical structure. Detailed analysis of the secondary flows can be found in [4].

Further figures show comparisons between the uncorrected five-hole probe measurements, the corrected five-hole probe measurements and the cross hot-wire reference data. In Figure 8 and Figure 9 the vertical and lateral velocity components are compared respectively. For the vertical velocity the uncorrected five-hole probe measurements demonstrate significant deviation from the reference data in the zone of the vane wake. The gradient $\partial U / \partial y$ is strongest in the wake and responsible for the discrepancy, however after the correction this discrepancy disappears. The correction is improving the result significantly, and the differences between the corrected five-hole probe measurements and the cross hotwire data are of the order of measurement uncertainty. From Figure 8 one can observe that the gradient $\partial U / \partial z$ is responsible for the erroneous measurement of W-component by the five-hole pressure probe. The largest discrepancy is seen in the sidewall boundary layer and in the vortex at z = -0.05. At these locations the variations of the streamwise velocity are significant in the lateral direction, see Figure 7. The lateral velocity data are visibly improved in these problematic areas after the correction. It can be noted that even though the correction calibration was performed with respect to V velocity component the correction performance is very good for W-component due to the probe symmetry.

For a deeper quantitative analysis the velocity profiles were extracted across the vane pitch at the spanwise locations highlighted in Figure 8 and Figure 9 by lines. These profiles are shown in Figure 10 and Figure 11. The figures depict the vertical and the lateral velocity components, respectively, at stations with z equal to -0.016, -0.036, and -0.060 m. Shown data sets demonstrate the remarkably good overall efficiency of the correction. As is seen the correction always affects the results in a positive way. Furthermore, a more thorough analysis at other measurement stations for other x/C locations did not reveal any negative effects from the applied correction; the measurement accuracy was always improved. In both Figure 10 and Figure 11 one can observe some remained discrepancies for velocities, however these differences are of the order of experimental uncertainty and it is difficult to judge if the discrepancies are caused by the hot-wire or pressure probe errors. It can be noted that in these stations the crossflow velocity components have nearly equal magnitudes (see Figure 7), however it is not clear if this effect influences the five-hole probe or the cross hot-wire measurements.

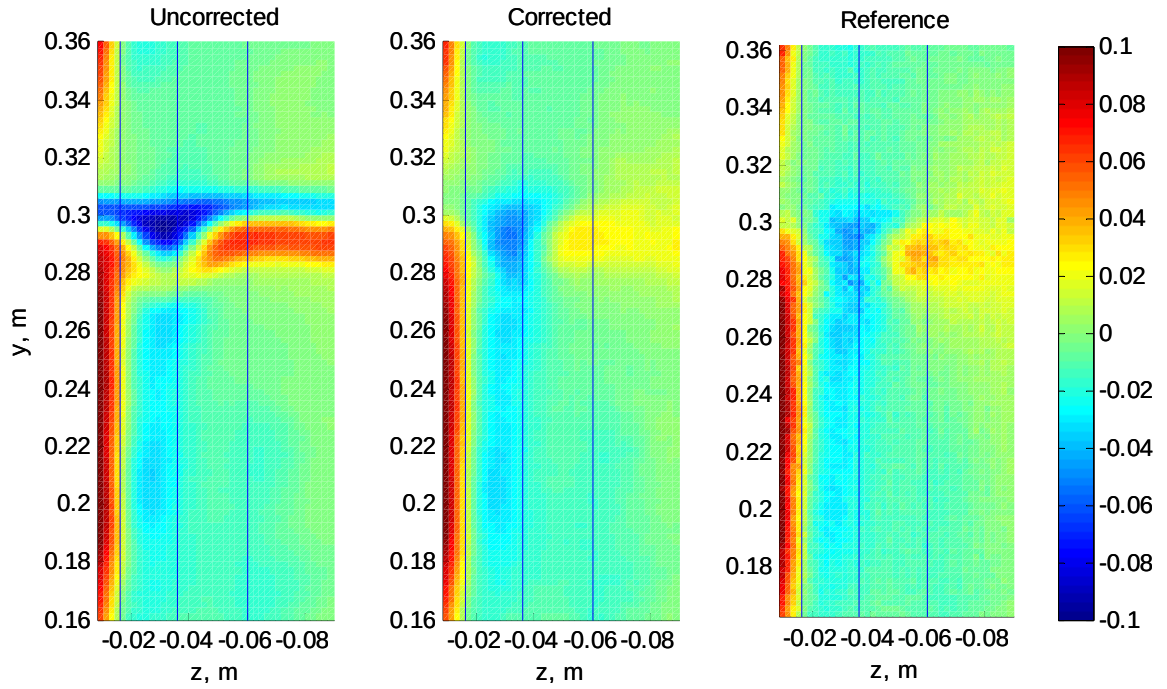

Figure 8 Contours of vertical velocity component V/U_{FS} at $x = 0.5C$. From left to right shown: uncorrected 5-hole probe measurements, corrected 5-hole probe measurements, and cross hot-wire measurements.

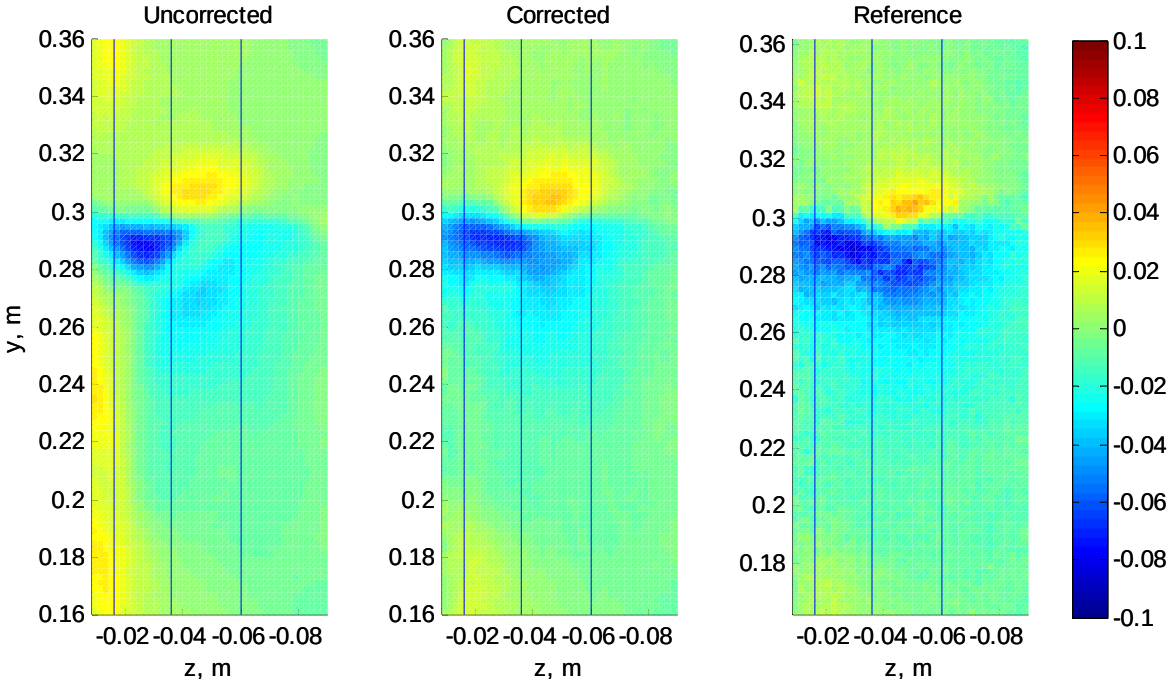

Figure 9 Contours of lateral velocity component W/U_{FS} at $x = 0.5C$. From left to right shown: uncorrected 5-hole probe measurements, corrected 5-hole probe measurements, and cross hot-wire measurements

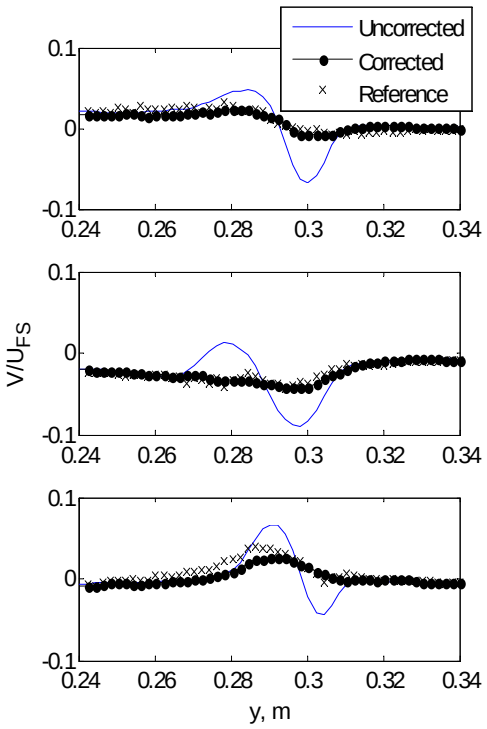

Figure 10 Profiles of vertical velocity component V/U_{FS} at x = 0.5C. z = -0.016, -0.036, -0.060 m (from top to bottom).

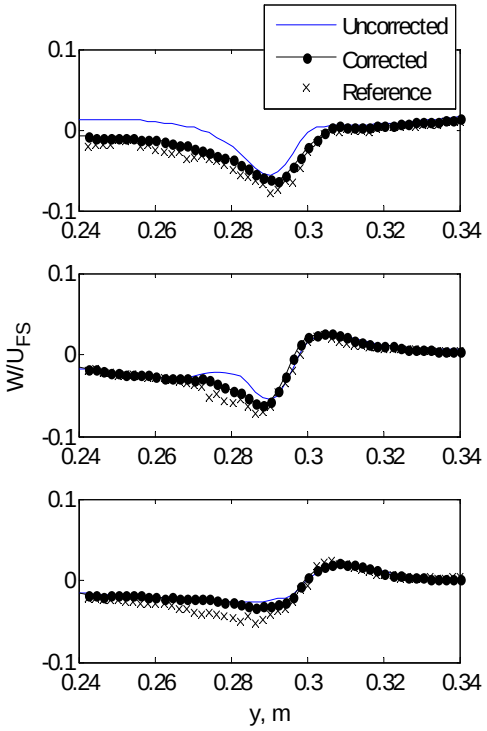

Figure 11 Profiles of lateral velocity component W/U_{FS} at x = 0.5C., z = -0.016, -0.036, -0.060 m (from top to bottom).

The secondary flow analysis assumes that the flow structures must be resolved accurately. The more accurate measurements of the crossflow velocity components will result in more accurately resolved flow streamlines as well. In Figure 12 the example of this positive effect of the correction is illustrated. One can observe that the uncorrected flow streamlines can reflect an unphysical behavior. The motion of the vortical structures in the leftmost diagram of Figure 12 is not described correctly. The corrected data are though in excellent agreement with the reference diagram.

From Figure 12 it can also be noted that the finite size effects of pressure probe do not influence the resultant streamwise vorticity. This result is not surprising and can be predicted from the character of the correction. From Eqs. (1) and (2) one can derive expressions for the measured velocities

$$V_{meas} = V - \Delta \frac{\partial U}{\partial y} \qquad \text{and} \qquad W_{meas} = W - \Delta \frac{\partial U}{\partial z}.$$

After this the streamwise vorticity estimated from the measured velocities without the correction can be obtained

$$\omega_{x,meas} = \frac{\partial W}{\partial y} - \frac{\partial V}{\partial z} - \Delta\left(\frac{\partial^2 U}{\partial y \partial z} - \frac{\partial^2 U}{\partial y \partial z}\right) = \frac{\partial W}{\partial y} - \frac{\partial V}{\partial z} = \omega_x$$

As one can immediately conclude, this behavior is only valid for axisymmetric probes, and provides an excellent opportunity to represent the multihole probe data in vorticities and exclude the finite size effects from experimental results automatically.

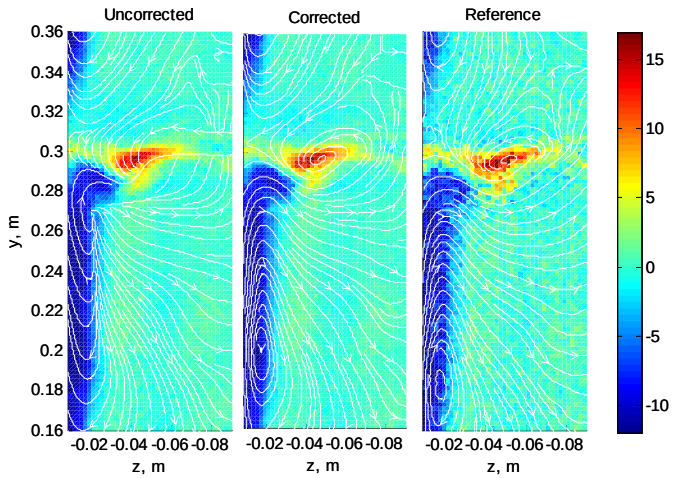

Figure 12 Contours of streamwise vorticity ω_x/U_{FS} at x = 0.5C with superimposed crossflow streamlines.

Finally, some results from the case with low turbulent inflow conditions are shown in Figures 13 and 14. The profiles of the vertical and lateral velocity components demonstrate that the improvement of the corrected data was obtained in this case as well. The very good performance of the correction can be noticed again.

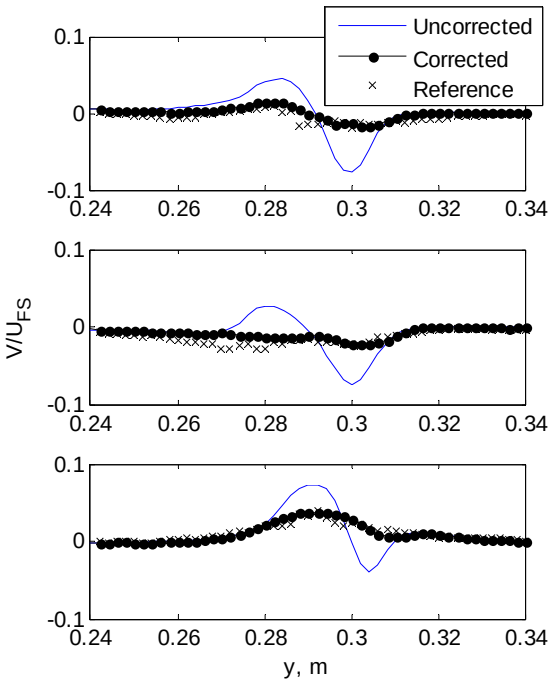

Figure 13 Case of low inlet turbulence. Profiles of vertical velocity component V/U_{FS} at x = 0.5C. z = -0.016, -0.036, -0.060 m (from top to bottom).

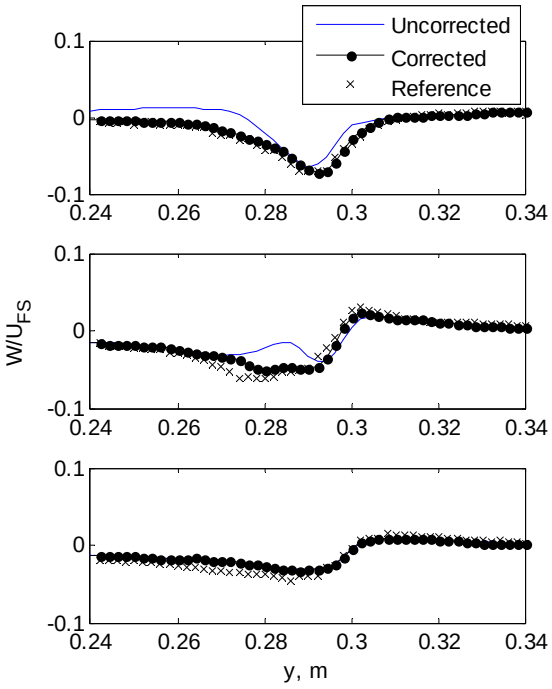

Figure 14 Case of low inlet turbulence. Profiles of lateral velocity component W/U_{FS} at x = 0.5C. z = -0.016, -0.036, -0.060 m (from top to bottom).

6 CONCLUDING REMARKS

The effect of the modified correction by Ligrani *et al.* [1] is scrutinized through detailed side-by-side comparison with corresponding cross hot-wire data. For highly three-dimensional flow the influence of the correction on all three velocity components, flow streamlines and streamwise vorticity fields is thoroughly examined. It is shown that the correction procedure can be implemented in two steps as in Ligrani *et al.* [1] or in a single step, either for probe pressures, or for velocity components. The correction for the velocity components is found to have the best performance. The present study demonstrates a very good efficiency and reliability of the correction, which lead to a significant improvement of the corrected velocity data. The improvement for the crossflow velocity components has allowed description of the flow streamlines correctly, and as a result, the secondary flow field structures were resolved more accurately. It is demonstrated that the streamwise vorticity derived from the measured five-hole probe velocities is not affected by the velocity gradient effects if the probe is axisymmetric. This provides an excellent opportunity to represent the multihole probe data in vorticities and exclude the finite size effects from the final result.

A very important fact is that the correction is not found to over-correct and distort the data, thus can be used safely. A very good performance of the correction for the finite-size effects of pressure probes presented in this study allows to recommend it as a mandatory step in postprocessing procedures for multihole pressure probes.

7 REFERENCES

[1] Ligrani P.M., Singer B.A., Baun L.R., 1989, "Spatial Resolution and Downwash Velocity Corrections for Multiple-Hole Pressure Probes in Complex Flows", *Exp. Fluids*, Vol. **7**, pp. 424-426.

[2] Hjärne, J., Chernoray, V., Larsson, J., Löfdahl, L., 2006, "An experimental investigation of secondary flows and loss development downstream of a highly loaded low pressure turbine outlet guide vane cascade", *ASME paper* GT2006-90561.

[3] Hjärne J., Chernoray V., Larsson J., Löfdahl L., 2007, "Numerical Validations of Secondary Flows and Loss Development Downstream of a Highly Loaded Low Pressure Turbine Outlet Guide Vane Cascade", *ASME paper* GT2007-27712.

[4] Hjärne J., 2007, "Turbine Outlet Guide Vane Flows", *PhD Thesis*, Chalmers University of Technology, Göteborg, Sweden.

[5] Kennedy S., 2006, "Secondary Flow Measurement of an Outlet Guide Vane Cascade at Low and High Inlet Turbulence Intensities", *Master Thesis*, Chalmers University of Technology / Queens University of Belfast.

[6] Kennedy, S., Chernoray, V., Hjärne, J., 2006, "Secondary flow measurement of an outlet guide vane cascade at low and high inlet turbulence intensities", *Proc. of the 6th Euromech Fluid Mechanics Conference*, Stockholm, Sweden, p. 38.

[7] Sieverding C.H., Arts T., Denos R., Brouckaert J.F., 2000, "Measurement techniques for unsteady flows in turbomachines", *Exp. Fluids*, Vol. **28**, No. 4, pp. 285-321.

[8] Allen, R., Traub, L., Johansen, E. S., Rediniotis, O. K. and Tsao, T., 2000, "A MEMS-Based 5-Sensor Probe", AIAA-2000-252.

[9] Ciocan, G. D., Vonnez, F., Baudoin, J. and Kueny, J., 1998, "Unsteady Five-Sensor Probe Development for Hydraulic Machinery", In Proc. of ASME Fluids Eng. Summer Meeting, Washington DC.

[10] Rediniotis, O. K., Johansen, E. S., Tsao, T., Seifert, A. and Pack, L. G., 1999, "MEMS-Based Probes for Velocity and Pressure Measurements in Unsteady and Turbulent Flowfields", AIAA-99-0521.

[11] Ramakrishnan, V. and Rediniotis, O.K., 2007, "Development of a 12-Hole Omnidirectional Flow-Velocity Measurement Probe", *AIAA J.*, Vol. **45**, No. 6, pp. 1430-1432.

[12] Hjärne, J., Chernoray, V., Larsson, J., 2008, "Experimental Investigations with Numerical Validation of a Low Pressure Turbine Outlet Guide Vane with a Simulated Engine Mount Recess", *ASME paper* GT2008-50168.

[13] Hjärne, J., Larsson, J. and Löfdahl, L., 2003, "Design of a Modern Test-Facility for LPT/OGV flows", *ASME paper* GT2003-38083.

[14] Hjärne, J., Larsson, J. and Löfdahl, L., 2005, "Experimental Evaluation of the Flow Field in a State of the Art Linear Cascade with Boundary-Layer Suction", *ASME paper* GT2005-68399.

[15] Hjärne, J., Chernoray, V., Larsson, J., Löfdahl, L., 2005, "Experimental analysis of the flow-field in a state-of-the-art linear cascade with boundary-layer suction", *ASME paper* GT2005-68399.

[16] Arts, T., Boerrigter, H., Buchlin, J.-M., Carbonaro, M., Degrez, G., Dénos, R., Fletcher, D., Olivari, D., Riethmuller, M.L., Van den Braembussche, R.A., "Measurement Techniques in Fluid Mechanics", 2nd revised edition, *reprint of VKI* LS 1994-01.

[17] Pisasale, A.J. and Ahmed, N.A., 2002, "Theoretical calibration for highly three-dimensional low-speed flows of a five-hole probe", *Meas. Sci. Technol.*, Vol. **13**, pp. 1100-1107.

[18] Cheng, M., Whyte, D.S., Lou, J., 2007, "Numerical simulation of flow around a square cylinder in uniform-shear flow", *J. Fluid. Struct.*, Vol. **23**, pp. 207-226.